Relating strain amplitude, strain threshold and bone formation rate to exogenous forcing frequency

Jitendra Prasad,

Department of Mechanical Engineering,

Indian Institute of Technology Ropar,

Rupnagar, Punjab, India - 140001.

Email: jprasad@iitrpr.ac.in

ORCID: 0000-0001-6389-955X

Abstract

The literature supports the existence of a strain threshold, above which cortical bone adapts to exogenous mechanical loading by forming new bone. This strain threshold, however, varies with loading conditions, locations, waveforms, frequency etc. and there is a need to mathematically express the strain threshold in terms of these parameters. There have been several parametric, mathematical or numerical models in the literature for the cortical bone's adaptation to mechanical loading, which may be already fitting some of the experimental data; however, they may not be easily and confidently derived from the first principles. To fill the gap, this work has attempted to derive the corresponding bone formation rate (BFR) rather from the first principles, namely using the energy principles. The derived model has been compared to the existing parametric models and validated with respect to the diverse experimental data available in the literature. The developed model is able to not only predict the BFR, but also helps to understand the nature and possible mathematical form of the strain threshold for cortical bone's adaptation to mechanical loading.

Keywords: Strain threshold, Derivation, Bone formation rate, Viscous dissipation energy, Cortical bone adaptation

1. Introduction

It has been long established through Wolff's law, that the bone adapts to exogenous mechanical loading [1]. Frost's mechanostat theory proposed a strain threshold above which there is a new bone formation for the bone to adapt to an exogenous mechanical loading [2]. Strain threshold has been supported by many works in the literature [3]. This strain threshold was, however, found to vary with loading conditions, locations, loading waveform, frequency of loading etc. [4]–[10]. For example, the strain thresholds reported for the cantilever loading of mouse tibia, with trapezoidal loading waveform are about 650 με [4] and 850 με [5], with and without rest-inserted waveform, respectively. The strain threshold in case of four-point loading of rat tibia was found to be higher, such as 1050 με [6]. In case of ulnar axial loading, the strain threshold was found to vary with frequency, from about 1820 με to approximately 650 με as the frequency of the loading waveform increased from 1 Hz to 10 Hz [7]. For such loading, the threshold was also found to vary approximately between 1343 με and 3074 με depending on the location [8]. For axial loading of tibia, the strain threshold was found to be approximately 1100 με [9]. Bone formation rate (BFR) was further found to depend on axial preloads, with higher BFR for lower axial preload, possibly due to preload-dependent strain threshold [10].

Despite its complex nature, strain threshold is an important parameter to quickly ascertain if some physical intervention will induce new bone formation at all. Moreover, some bone adaptation models (e.g. [11], [12]) directly use strain thresholds to compute site-specific mineral apposition rate (MAR) or an average bone formation rate (BFR) at a bone cross-section. Accuracy of strain threshold will directly enhance accuracy of such adaptation models. While there has been strong evidence of strain threshold's

dependance on a number of parameters such as loading condition, location, loading waveform, frequency etc., there is no existing mathematical model in the literature that clearly and elegantly relates the strain threshold to these parameters. The present work attempts to fill the gap by deriving the strain threshold from first principles and validating with the experimental data.

The variable nature of the strain threshold may indicate that the mechanical strain may not be directly inducing new bone formation. There have been accordingly diverse mathematical or computer models of cortical bone's adaptation to mechanical loading. For example, thresholds for new bone formations have been popularly suggested in terms of strain-energy density [13]–[15]. Threshold of viscous dissipation energy can also be found in the literature for modeling bone adaptation [16]. Other kinds of thresholds in the literature include principal stress [13], fatigue damage accumulation [12], [13], strain rate (i.e. strain times frequency, [7], [17]), strain gradient [18], etc. As such, there is no consensus on the nature of threshold for loading-induced new bone formation. Derivation of threshold from first principles may help to identify the correct nature of the threshold and the current work is a step towards such identification.

The present work first proposes an equivalent thermodynamic model to derive how bone formation rate (BFR) can possibly be related to viscoelastic energy dissipated during loading. The derived model has been compared to existing models of bone adaptation and has been successfully validated using the experimental data in the literature (e.g. [7], [19]). The model brings out a mathematical expression of strain threshold as a direct or indirect function of loading, location, loading waveform, frequency, preload etc. The

obtained expression for strain threshold varies with the parameters, in accordance with the experimental data found in the literature.

The rest of the paper is organized as follows. Derivations of BFR and strain threshold are given in Section 2, i.e. the Methodology section. Related computational methodologies are also given in Section 2. The model has been validated and the results have been discussed in Section 3, i.e. the Results and Discussions section. The last section, i.e. Section 4 summarizes the findings and importance of this work.

2. Methodology

2.1. The 1D Poroelastic Model

Biot's [20] derived the settlement of the poroelastic column of height L subjected to a compressive stress of σ_0 as a function of time (t) as follows:

$$u(t) = -\frac{8}{\pi^2}(a - a_i)L\sigma_0 \sum_{n=0}^{inf} \frac{1}{(2n+1)^2} exp\left(-\left[\frac{(2n+1)\pi}{2L}\right]^2 ct\right) + aL\sigma_0 \quad (1)$$

where a = final compressibility, a_i = instantaneous compressibility and c = consolidation constant are properties of poroelastic material as defined by Biot [20].

Simplifying with n = 0 only,

$$u(t) = -\frac{8}{\pi^2}(a - a_i)L\sigma_0 exp\left(-\frac{\pi^2 ct}{4L^2}\right) + aL\sigma_0 \quad (2)$$

The corresponding creep is given by

$$h(t) = \frac{\epsilon(t)}{\sigma_0} = \frac{u(t)}{L\sigma_0} = a - \frac{8}{\pi^2}(a - a_i)exp\left(-\frac{\pi^2 ct}{4L^2}\right) \quad (3)$$

Taking Laplace Transform of the above:

$$H(s) = \frac{a}{s} - \frac{8}{\pi^2}(a - a_i)\frac{1}{s+\frac{\pi^2 c}{4L^2}} = \frac{a}{s} - \frac{8(a-a_i)/\pi^2}{(s+\frac{\pi^2 c}{4L^2})} \quad (4)$$

The corresponding modulus in frequency domain is

$$G(s) = \frac{1}{sH(s)} = \frac{(s+\frac{\pi^2 c}{4L^2})}{a(s+\frac{\pi^2 c}{4L^2})-8(a-a_i)s/\pi^2} = \frac{s+\pi^2 c/(4L^2)}{(a-8(a-a_i)/\pi^2)s+\pi^2 ca/(4L^2)} \tag{5}$$

or

$$G(s) = \frac{\pi^2}{(a\pi^2-8(a-a_i))}\frac{s+\pi^2 c/(4L^2)}{s+\pi^4 ca/(4L^2)/(a\pi^2-8(a-a_i))} = \frac{\tau_\sigma}{a\tau_\epsilon}\frac{s+1/\tau_\sigma}{s+1/\tau_\epsilon} \tag{6}$$

or

$$G(s) = \frac{\tau_\sigma s+1}{a(\tau_\epsilon s+1)} = E_0\frac{\tau_\sigma s+1}{\tau_\epsilon s+1} \tag{7}$$

where

$$\tau_\sigma = \frac{4L^2}{\pi^2 c} \tag{8}$$

$$\tau_\epsilon = \frac{4L^2(a\pi^2-8a+8a_i)}{\pi^4 ca} = \frac{\tau_\sigma(a\pi^2-8a+8a_i)}{a\pi^2} = \tau_\sigma(1 - \frac{8}{\pi^2} + \frac{8a_i}{a\pi^2}) \tag{9}$$

$$E_0 = \frac{1}{a} \tag{10}$$

The corresponding complex modulus is

$$G^*(\omega) = E_0\frac{1+i\omega\tau_\sigma}{1+i\omega\tau_\epsilon} = G'(\omega) + iG''(\omega) \tag{11}$$

where G' and G'' are storage and loss modulus, which are respectively real and imaginary parts of the complex modulus G^*.

$$G'(\omega) = E_0\frac{\omega^2\tau_\sigma\tau_\epsilon+1}{\omega^2\tau_\epsilon^2+1} \tag{12}$$

$$G''(\omega) = E_0\frac{\omega(\tau_\sigma-\tau_\epsilon)}{\omega^2\tau_\epsilon^2+1} \tag{13}$$

2.2. The Equivalent Viscoelastic Model

The Biot's poroelastic model is equivalent to the Standard Linear Solid model of viscoelasticity, whose stress-strain relation is given as follows [21]:

$$\sigma + \tau_{\epsilon}\dot{\sigma} = E_0(\epsilon + \tau_{\sigma}\dot{\epsilon}) \tag{14}$$

Hsieh et al (2009) presents the stress amplitude vs strain amplitude data for female Sprague-Dawley rats of age 7–8 months old when ulna is loaded with the Haversine loading waveform [19]. The corresponding experiment data may be fit to the viscoelastic model to determine the values of the constants τ_{ϵ} , τ_{σ} and E_0 .

In response to the Haversine waveform of stress:

$$\sigma(t) = \sigma_0(1 - cos(\omega t)) \tag{15}$$

With the stress amplitude $\sigma_0 > 0$, the corresponding steady-state strain will be of the form:

$$\epsilon = \frac{\sigma_0}{E_0} - \epsilon_0 cos(\omega t - \theta) \tag{16}$$

where

$$\epsilon_0 = \frac{\sigma_0}{|G^*(\omega)|} \tag{17}$$

and

$$\theta = tan^{-1}\frac{G''(\omega)}{G'(\omega)} \tag{18}$$

Thus, for the cyclic stress amplitude σ_0, the cyclic strain amplitude is given by:

$$\epsilon_0 = \frac{\sigma_0}{E_0}\frac{\sqrt{1+\tau_{\epsilon}^2\omega^2}}{\sqrt{1+\tau_{\sigma}^2\omega^2}} \tag{19}$$

The experimentally-reported peak stress is typically the peak-to-trough amplitude of the strain. The peak strain is thus given by:

$$\epsilon_{peak} = 2\epsilon_0 = \frac{2\sigma_0}{E_0}\frac{\sqrt{1+\tau_\epsilon^2\omega^2}}{\sqrt{1+\tau_\sigma^2\omega^2}} = \epsilon_{peak}^0\frac{\sqrt{1+\tau_\epsilon^2\omega^2}}{\sqrt{1+\tau_\sigma^2\omega^2}} \quad (20)$$

where ϵ_{peak}^0 is the peak strain at zero frequency (or very-very low frequency).

The Levenberg-Marquardt Algorithm implemented through MATLAB (Mathworks Inc.) has been used for the curve fitting and determining the values of the constants τ_ϵ , τ_σ and ϵ_{peak}^0 [22], [23]. The Chi-Square Goodness of Fit (i.e. Pearson's chi-squared test) has been used to quantify the quality of curve-fitting [24].

2.3. Derivation of Strain Threshold

According to the First Law of Thermodynamics [25],

$$dQ = dU + dW \quad (21)$$

where dQ is the energy supplied to a system, dU is the change in the internal energy of the system and dW is the work done by the system.

For one cycle of loading,

$$\oint dQ = \oint dU + \oint dW \quad (22)$$

However, for a cyclic loading, the net change in the internal energy is zero, i.e.

$$\oint dU = 0 \quad (23)$$

Thus,

$$\oint dQ = \oint dW \tag{24}$$

Let ϕ be the energy supplied to per unit volume of the loaded bone, then

$$\phi = \oint dq = \oint dw = \int_0^T \sigma(t)\frac{d\epsilon}{dt}dt \tag{25}$$

where dq is the energy supplied per unit volume of the system, dw is the work done per unit volume the system and T is the time period of the cyclic loading. The quantity ϕ is called the dissipation energy density [26].

Using the expressions for $\sigma(t)$ and $\epsilon(t)$ given in Section 2.2, in accordance with [26], [27], we get

$$\phi = \pi G''(\omega)\epsilon_0^2 \tag{26}$$

Using the expressions for $G''(\omega)$ given in Section 2.2, we get

$$\phi = \frac{\omega(\tau_\sigma - \tau_\epsilon)\pi E_0 \epsilon_0^2}{\omega^2 \tau_\epsilon^2 + 1} \tag{27}$$

Assuming that the dissipation energy density (ϕ) must exceed a threshold value for new bone formation,

$$\phi > \phi_{thres} \tag{28}$$

or

$$\epsilon_0 > \sqrt{\frac{\phi_{thres}(\omega^2 \tau_\epsilon^2 + 1)}{\omega(\tau_\sigma - \tau_\epsilon)\pi E_0}} \tag{29}$$

or

$$2\epsilon_0 > 2\sqrt{\frac{\phi_{thres}(\omega^2\tau_\epsilon^2+1)}{\omega(\tau_\sigma-\tau_\epsilon)\pi E_0}} \tag{30}$$

or

$$\epsilon_{peak} > \epsilon_{thres} \tag{31}$$

where

$$\epsilon_{thres} = 2\sqrt{\frac{\phi_{thres}(\omega^2\tau_\epsilon^2+1)}{\omega(\tau_\sigma-\tau_\epsilon)\pi E_0}} \tag{32}$$

The existing experimentally determined strain threshold data (by Hsieh et al [7]) has been fitted to the derived strain threshold using the Levenberg-Marquardt Algorithm ([22], [23]) to determine the value of ϕ_{thres} . MATLAB software (Mathworks Inc.) has been used for the curve-fitting.

2.4. Derivation of Bone Formation Rate (BFR)

It is assumed that when loading on the bones changes, the bone will do as needed (such as changing the shape and size of the bone cross-section) to attain ϕ_{thres} as the final dissipation energy density. As in Section 2.3,

$$\phi = \frac{\omega(\tau_\sigma-\tau_\epsilon)\pi E_0\epsilon_0^2}{\omega^2\tau_\epsilon^2+1} \tag{33}$$

Expressing the stress σ in terms of axial force and induced moments, we get

$$\sigma(x,y,t) = \frac{F_z(t)}{A} - \left(\frac{I_{xx}M_y(t)+I_{xy}M_x(t)}{I_{xx}I_{yy}-I_{xy}^2}\right)x + \left(\frac{I_{yy}M_x(t)+I_{xy}M_y(t)}{I_{xx}I_{yy}-I_{xy}^2}\right)y \tag{34}$$

Assuming the following, which is approximately true for a section in concern:

$$I_{xx} = A\alpha^2 \tag{35}$$

$$I_{yy} = A\beta^2 \tag{36}$$

$$I_{xy} = A\gamma^2 \tag{37}$$

$$M_x = F_z \delta_y \tag{38}$$

$$M_y = F_z \delta_x \tag{39}$$

where α, β, γ, δ_x and δ_y are constants.

$$\sigma(x, y, t) = \frac{F_z(t)}{A}\left[1 - \left(\frac{\alpha^2\delta_x + \gamma^2\delta_y}{\alpha^2\beta^2 - \gamma^4}\right)x + \left(\frac{\beta^2\delta_y + \gamma^2\delta_x}{\alpha^2\beta^2 - \gamma^4}\right)y\right] \tag{40}$$

As stress σ is cyclic, having the Haversine waveform [7], the stress amplitude is given by:

$$\sigma_0 = \lambda\frac{F_0}{A} \tag{41}$$

where

$$\lambda = 1 - \left(\frac{\alpha^2\delta_x + \gamma^2\delta_y}{\alpha^2\beta^2 - \gamma^4}\right)x_0 + \left(\frac{\beta^2\delta_y + \gamma^2\delta_x}{\alpha^2\beta^2 - \gamma^4}\right)y_0 \tag{42}$$

is a constant. F_0 is the force amplitude of the cyclic loading.

$$\epsilon_0 = \lambda\frac{F_0}{A|G^*(\omega)|} \tag{43}$$

Accordingly,

$$\phi = \frac{\omega(\tau_\sigma - \tau_\epsilon)\pi E_0}{\omega^2\tau_\epsilon^2 + 1}\frac{\lambda^2 F_0^2}{A^2|G^*(\omega)|^2} \tag{44}$$

or

$$\phi A^2 = \frac{\omega(\tau_\sigma - \tau_\epsilon)\pi E_0}{\omega^2 \tau_\epsilon^2 + 1} \frac{\lambda^2 F_0^2}{|G^*(\omega)|^2} \tag{45}$$

For the same section and for the same loading protocol (including the number of cycles per day),

$$\phi A^2 = \xi(\omega) \tag{46}$$

where ξ is a function of frequency ω, given by

$$\xi(\omega) = \frac{\omega(\tau_\sigma - \tau_\epsilon)\pi E_0}{\omega^2 \tau_\epsilon^2 + 1} \frac{\lambda^2 F_0^2}{|G^*(\omega)|^2} \tag{47}$$

or

$$A = \sqrt{\frac{\xi(\omega)}{\phi}} \tag{48}$$

Bone Formation Rate (BFR) may be derived similar to the Mineral Apposition Rate (MAR) derived in Singh et al [27]. According, rate of change of area is assumed to be proportional to the difference between the final area of cross-section and the current area of cross-section, i.e.

$$\frac{dA}{dt} \propto (A_f - A) \tag{49}$$

or

$$\frac{dA}{dt} = (A_f - A)\zeta \tag{50}$$

where ζ is the proportionality constant, which may be a function of the loading condition / protocol (including the number of cycles of loading per day). This equation may be rewritten in terms of dissipation energy density as

$$\frac{dA}{dt} = (A_f - A)\zeta \tag{51}$$

or

$$\frac{dA}{dt} = (\sqrt{\frac{\xi(\omega)}{\phi_f}} - \sqrt{\frac{\xi(\omega)}{\phi}})\zeta \tag{52}$$

or

$$\frac{dA}{dt} = (\sqrt{\frac{\xi(\omega)}{\phi_f}} - \sqrt{\frac{\xi(\omega)}{\phi}})\zeta \tag{53}$$

or

$$\frac{dA}{dt} = (\sqrt{\phi} - \sqrt{\phi_f})\frac{\zeta}{\sqrt{\phi_f}}\sqrt{\frac{\xi(\omega)}{\phi}} \tag{54}$$

or

$$\frac{dA}{dt} = (\sqrt{\phi} - \sqrt{\phi_f})\frac{\zeta A}{\sqrt{\phi_f}} \tag{55}$$

The bone formation rate (BFR) is given by,

$$BFR = \frac{1}{s_b}\frac{dA}{dt} = (\sqrt{\phi} - \sqrt{\phi_f})\frac{1}{s_b}\frac{\zeta A}{\sqrt{\phi_f}} \tag{56}$$

where s_b is the bone surface (BS), i.e. perimeter of the bone section.

Or,

$$BFR = B(\sqrt{\phi} - \sqrt{\phi_f}) \tag{57}$$

where B is approximately a constant given by

$$B = \frac{1}{s_b}\frac{\zeta A}{\sqrt{\phi_f}} \tag{58}$$

The BFR may be rewritten as

$$BFR = B(\sqrt{\phi} - \sqrt{\phi_f}) \tag{59}$$

$$BFR = \frac{B}{2}\left[\frac{\omega(\tau_\sigma - \tau_\epsilon)\pi E_0}{\omega^2\tau_\epsilon^2 + 1}\right]^{\frac{1}{2}}(\epsilon_{peak} - \epsilon_{thres}) \tag{60}$$

Hsieh and Turner [7] provided the experimental BFR data which varied with frequency. The Levenberg-Marquardt Algorithm ([22], [23]) has been used to fit the experimental data to the above mathematical model for BFR and accordingly determine the value of B.

3. Results and Discussions

3.1. Peak Strain as a Function of Frequency

As derived in Section 2.2,

$$\epsilon_{peak} = \epsilon_{peak}^0 \frac{\sqrt{1+\tau_\epsilon^2\omega^2}}{\sqrt{1+\tau_\sigma^2\omega^2}} \tag{61}$$

Curve fitting determined the following values of parameters: ϵ_{peak}^0 = 168 με, τ_σ = 0.0449 s, and τ_ϵ = 0. The peak strain is plotted in Fig. 1 using a solid line, where the experimental

peak strains are shown as circles. Chi Square Goodness of Fit analysis has been carried out [24]. The p-value is found to be 0.99, which indicates that the mathematical model is significantly the same as that of the experimental findings.

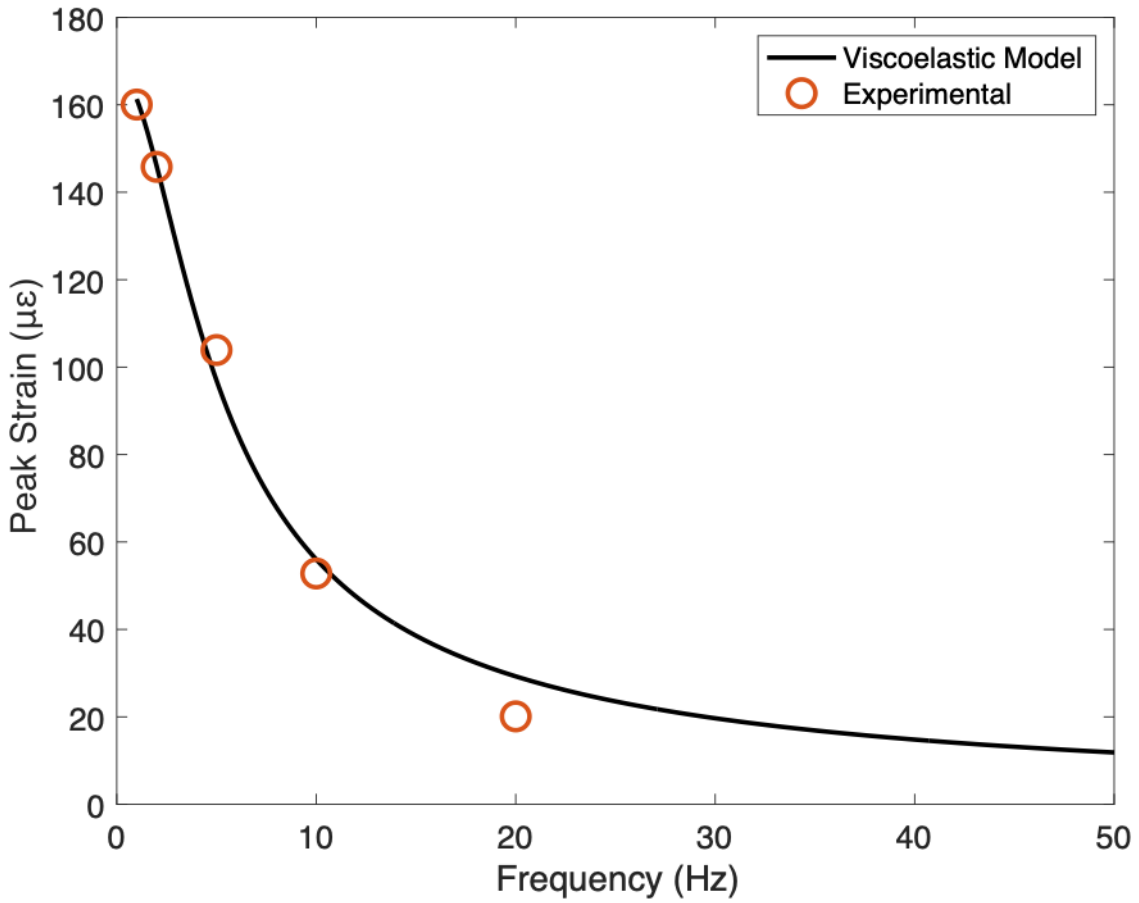

Figure 1. Peak strain versus forcing frequency.

Note that with $\tau_\epsilon = 0$, the peak strain is thus simplifies to

$$\epsilon_{peak} = \frac{\epsilon^0_{peak}}{\sqrt{1+\tau_\sigma^2\omega^2}} \tag{62}$$

The Linear Elastic Solid viscoelastic model now simplifies to the Kelvin-Voigt model [12], [21].

3.2. Strain Threshold as a Function of Frequency

As per Section 2.3, the strain threshold is given by

$$\epsilon_{thres} = 2\sqrt{\frac{\phi_{thres}(\omega^2\tau_\epsilon^2+1)}{\omega(\tau_\sigma-\tau_\epsilon)\pi E_0}} \tag{63}$$

Setting $\tau_\epsilon = 0$ in the above equation, we get

$$\epsilon_{thres} = 2\sqrt{\frac{\phi_{thres}}{\pi E_0 \omega \tau_\sigma}} \tag{64}$$

or

$$\epsilon_{thres} = \frac{C}{\sqrt{f}} \tag{65}$$

where

$$C = \sqrt{\frac{2\phi_{thres}}{\pi^2 E_0 \tau_\sigma}} \tag{66}$$

is a constant.

After the least squares curve-fitting, the value of C is found to be 1838 με-s. The predicted strain threshold as a function of forcing frequency is shown in Fig. 2. The experimental strain threshold is shown as squares in the figure. The p-value for the Chi-Square Goodness of Fit test is 0.955 (i.e. $p > 0.95$), which means that the results of the mathematical model are not significantly different from the experimental results.

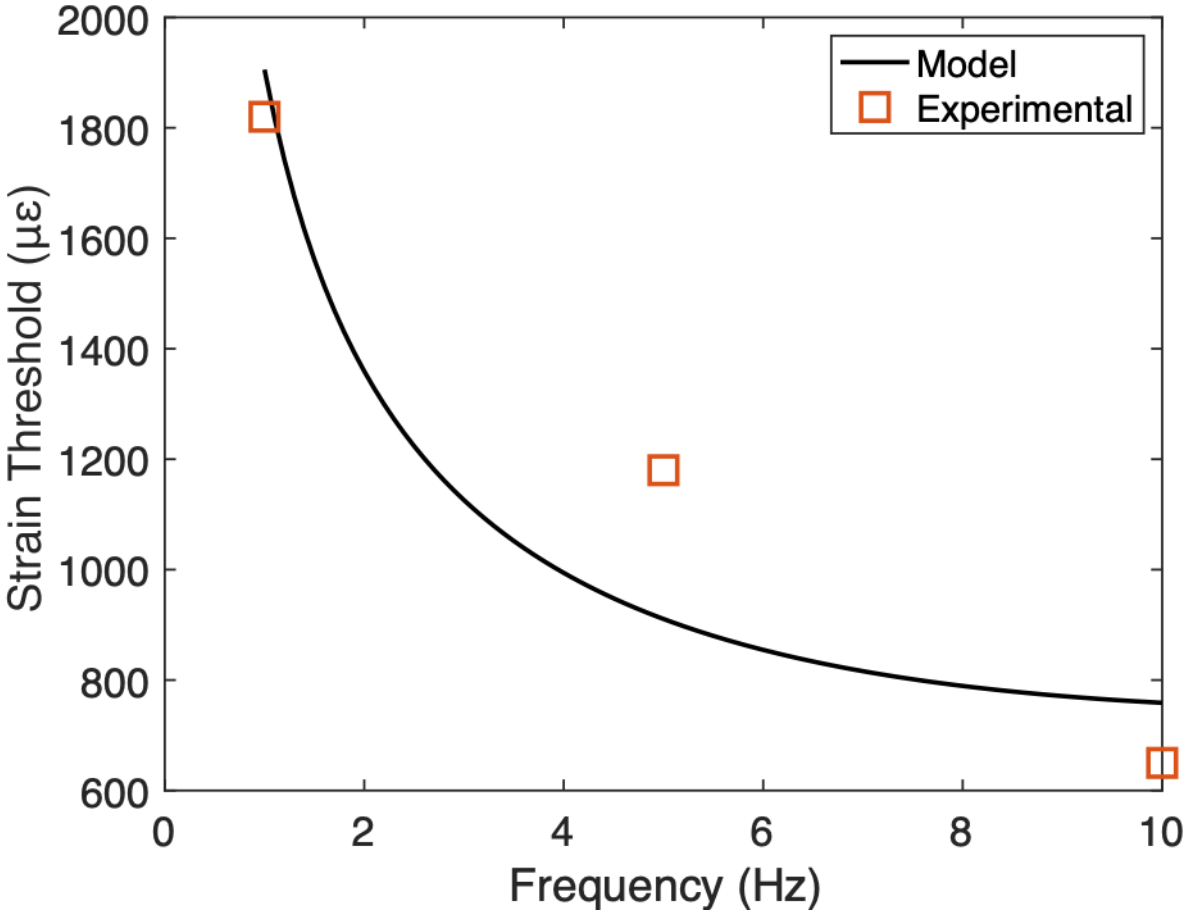

Figure 2. Strain threshold as a function of forcing frequency.

3.3. Bone Formation Rate (BFR) as a Function of Frequency

As derived in Section 2.4, the Bone Formation Rate (BFR) is given as follows:

$$BFR = \frac{B}{2}\left[\frac{\omega(\tau_\sigma - \tau_\epsilon)\pi E_0}{\omega^2\tau_\epsilon^2 + 1}\right]^{\frac{1}{2}}(\epsilon_{peak} - \epsilon_{thres}) \tag{67}$$

Setting $\tau_\epsilon = 0$, the BFR is given by

$$BFR = \frac{B\sqrt{\omega\tau_\sigma\pi E_0}}{2}(\epsilon_{peak} - \epsilon_{thres}) \tag{68}$$

or

$$BFR = D(\epsilon_{peak} - \epsilon_{thres})\sqrt{f} \tag{69}$$

where

$$D = B\pi\sqrt{\tau_{\sigma} E_0/2} \tag{70}$$

is a constant.

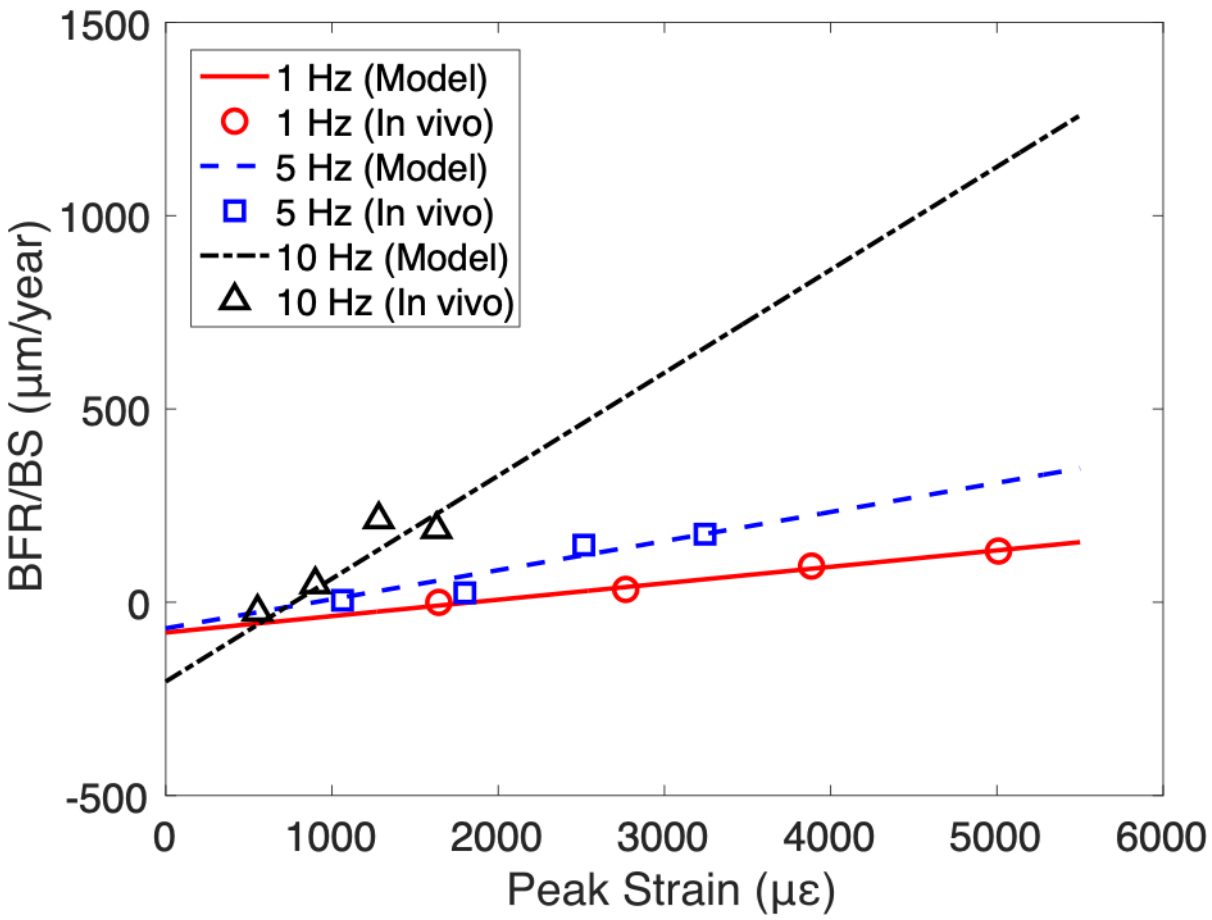

Figure 3. Bone Formation Rate (BFR/BS) as a function of peak strain.

The least squares curve fitting finds the following values of constant D for the three frequencies 1Hz, 5Hz and 10Hz respectively: 0.0425, 0.0337, and 0.0842 μm-$s^{1/2}$/με, which are approximately of the same order.

The BFR predicted by the mathematical model is shown as a red solid line, blue dashed line and black dash-dotted line, respectively, for the forcing frequencies 1 Hz, 5 Hz and 10 Hz. The corresponding experimental data are shown as red circles, blue squares and red triangles, respectively. The p-values for the Chi-Square Goodness of Fit test are 0.9809, 0.1524 and 0.8874, respectively, which mean that the mathematical model prediction is not significantly different from the experimental values.

4. Conclusions

This study derives peak strain, strain threshold and bone formation rate (BFR) from basic principles for the first time and successfully validates against the existing experimental data. The work theoretically establishes for the first time that (i) Dissipation energy density is maintained at a universal constant value in bone, (ii) If the dissipation energy density is disturbed by application of increased forces on bone, the bone acts to bring the dissipation energy density to the universal value, (iii) The corresponding bone formation rate (BFR) is proportional to increase in the square root of dissipation energy density from corresponding universal value, (iv) BFR slowly decreases to zero as dissipation energy density slowly approaches the universal value.

Declarations:

Conflicts of interest/Competing interests: None

Availability of data and material: The data are taken from the previously published journal articles and hence publicly available.

References

[1] J. Wolff, "Ueber die innere Architectur der Knochen und ihre Bedeutung für die Frage vom Knochenwachsthum," *Arch. Für Pathol. Anat. Physiol. Für Klin. Med.*, vol. 50, pp. 389–450, 1870.

[2] H. M. Frost, "Bone 'mass' and the 'mechanostat': a proposal," *Anat. Rec.*, vol. 219, no. 1, pp. 1–9, Sep. 1987, doi: 10.1002/ar.1092190104.

[3] C. T. Rubin and L. E. Lanyon, "Regulation of bone mass by mechanical strain magnitude," *Calcif. Tissue Int.*, vol. 37, no. 4, pp. 411–417, Jul. 1985, doi: 10.1007/BF02553711.

[4] S. Srinivasan, B. J. Ausk, S. L. Poliachik, S. E. Warner, T. S. Richardson, and T. S. Gross, "Rest-inserted loading rapidly amplifies the response of bone to small increases in strain and load cycles," *J. Appl. Physiol. Bethesda Md 1985*, vol. 102, no. 5, pp. 1945–1952, May 2007, doi: 10.1152/japplphysiol.00507.2006.

[5] S. Srinivasan, D. A. Weimer, S. C. Agans, S. D. Bain, and T. S. Gross, "Low-magnitude mechanical loading becomes osteogenic when rest is inserted between each load cycle," *J. Bone Miner. Res. Off. J. Am. Soc. Bone Miner. Res.*, vol. 17, no. 9, pp. 1613–1620, Sep. 2002, doi: 10.1359/jbmr.2002.17.9.1613.

[6] C. H. Turner, M. R. Forwood, J. Y. Rho, and T. Yoshikawa, "Mechanical loading thresholds for lamellar and woven bone formation," *J. Bone Miner. Res. Off. J. Am. Soc. Bone Miner. Res.*, vol. 9, no. 1, pp. 87–97, Jan. 1994, doi: 10.1002/jbmr.5650090113.

[7] Y. F. Hsieh and C. H. Turner, "Effects of loading frequency on mechanically induced bone formation," *J. Bone Miner. Res. Off. J. Am. Soc. Bone Miner. Res.*, vol. 16, no. 5, pp. 918–924, May 2001, doi: 10.1359/jbmr.2001.16.5.918.

[8] Y. F. Hsieh, A. G. Robling, W. T. Ambrosius, D. B. Burr, and C. H. Turner, "Mechanical loading of diaphyseal bone in vivo: the strain threshold for an osteogenic response varies with location," *J. Bone Miner. Res. Off. J. Am. Soc. Bone Miner. Res.*, vol. 16, no. 12, pp. 2291–2297, Dec. 2001, doi: 10.1359/jbmr.2001.16.12.2291.

[9] T. Sugiyama, L. B. Meakin, W. J. Browne, G. L. Galea, J. S. Price, and L. E. Lanyon, "Bones' adaptive response to mechanical loading is essentially linear between the low strains associated with disuse and the high strains associated with the lamellar/woven bone transition," *J. Bone Miner. Res. Off. J. Am. Soc. Bone Miner. Res.*, vol. 27, no. 8, pp. 1784–1793, Aug. 2012, doi: 10.1002/jbmr.1599.

[10] S. Srinivasan *et al.*, "Static Preload Inhibits Loading-Induced Bone Formation," *JBMR Plus*, vol. 3, no. 5, p. e10087, May 2019, doi: 10.1002/jbm4.10087.

[11] S. Srinivasan *et al.*, "Rescuing Loading Induced Bone Formation at Senescence," *PLoS Comput. Biol.*, vol. 6, no. 9, p. e1000924, Sep. 2010, doi: 10.1371/journal.pcbi.1000924.

[12] J. Prasad and A. Goyal, "An Invertible Mathematical Model of Cortical Bone's Adaptation to Mechanical Loading," *Sci. Rep.*, vol. 9, no. 1, p. 5890, Apr. 2019, doi: 10.1038/s41598-019-42378-5.

[13] D. R. Carter, D. P. Fyhrie, and R. T. Whalen, "Trabecular bone density and loading history: regulation of connective tissue biology by mechanical energy," *J. Biomech.*, vol. 20, no. 8, pp. 785–794, 1987, doi: 10.1016/0021-9290(87)90058-3.

[14] A. G. Robling and C. H. Turner, "Mechanical signaling for bone modeling and remodeling," *Crit. Rev. Eukaryot. Gene Expr.*, vol. 19, no. 4, pp. 319–338, 2009, doi: 10.1615/critreveukargeneexpr.v19.i4.50.

[15] A. K. Tiwari and J. Prasad, “Computer modelling of bone’s adaptation: the role of normal strain, shear strain and fluid flow,” *Biomech. Model. Mechanobiol.*, vol. 16, no. 2, pp. 395–410, Apr. 2017, doi: 10.1007/s10237-016-0824-z.
[16] C. Kumar, I. Jasiuk, and J. Dantzig, “Dissipation energy as a stimulus for cortical bone adaptation,” *J. Mech. Mater. Struct.*, vol. 6, no. 1–4, pp. 303–319, Jun. 2011, doi: 10.2140/jomms.2011.6.303.
[17] C. H. Turner, “Three rules for bone adaptation to mechanical stimuli,” *Bone*, vol. 23, no. 5, pp. 399–407, Nov. 1998, doi: 10.1016/s8756-3282(98)00118-5.
[18] A. K. Tiwari, A. Goyal, and J. Prasad, “Modeling cortical bone adaptation using strain gradients,” *Proc. Inst. Mech. Eng. [H]*, vol. 235, no. 6, pp. 636–654, Jun. 2021, doi: 10.1177/09544119211000228.
[19] Y.-F. Hsieh, T. Wang, and C. H. Turner, “Viscoelastic response of the rat loading model: implications for studies of strain-adaptive bone formation,” *Bone*, vol. 25, no. 3, pp. 379–382, Sep. 1999, doi: 10.1016/S8756-3282(99)00181-7.
[20] M. A. Biot, “General Theory of Three-Dimensional Consolidation,” *J. Appl. Phys.*, vol. 12, no. 2, pp. 155–164, Feb. 1941, doi: 10.1063/1.1712886.
[21] C. R. Ethier and C. A. Simmons, *Introductory biomechanics: from cells to organisms*, 13th printing. in Cambridge texts in biomedical engineering. Cambridge: Cambridge University Press, 2018.
[22] K. Levenberg, “A method for the solution of certain non-linear problems in least squares,” *Q. Appl. Math.*, vol. 2, no. 2, pp. 164–168, 1944, doi: 10.1090/qam/10666.
[23] D. W. Marquardt, “An Algorithm for Least-Squares Estimation of Nonlinear Parameters,” *J. Soc. Ind. Appl. Math.*, vol. 11, no. 2, pp. 431–441, Jun. 1963, doi: 10.1137/0111030.
[24] K. Pearson, “On the criterion that a given system of deviations from the probable in the case of a correlated system of variables is such that it can be reasonably supposed to have arisen from random sampling,” *Lond. Edinb. Dublin Philos. Mag. J. Sci.*, vol. 50, no. 302, pp. 157–175, Jul. 1900, doi: 10.1080/14786440009463897.
[25] R. Clausius, “Ueber die bewegende Kraft der Wärme und die Gesetze, welche sich daraus für die Wärmelehre selbst ableiten lassen,” *Ann. Phys. Chem.*, vol. 155, no. 4, pp. 500–524, 1850, doi: 10.1002/andp.18501550403.
[26] J. R. Cho, H. W. Lee, W. B. Jeong, K. M. Jeong, and K. W. Kim, “Numerical estimation of rolling resistance and temperature distribution of 3-D periodic patterned tire,” *Int. J. Solids Struct.*, vol. 50, no. 1, pp. 86–96, Jan. 2013, doi: 10.1016/j.ijsolstr.2012.09.004.
[27] Sanjay Singh, Satwinder Jit Singh, and Jitendra Prasad, “Derivation, Validation, and Prediction of Loading-Induced Mineral Apposition Rates at Endocortical and Periosteal Bone Surfaces Based on Fluid Velocity and Pore Pressure,” *bioRxiv*, p. 2023.09.08.556956, Jan. 2023, doi: 10.1101/2023.09.08.556956.